

Anisotropy of the Universe via the Pantheon supernovae sample revisited

Dong Zhao^{1,2}, Yong Zhou^{1,2*} and Zhe Chang^{1,2}

¹*Institute of High Energy Physics, Chinese Academy of Sciences, Beijing 100049, China*

²*School of Physical Sciences, University of Chinese Academy of Sciences, Beijing 100049, China*

Accepted xxxx; Received xxxx; in original form xxxx

ABSTRACT

We employ the hemisphere comparison (HC) method and the dipole fitting (DF) method to investigate the cosmic anisotropy in the recently released Pantheon sample of type Ia supernovae (SNe Ia) and five combinations among Pantheon. For the HC method, we find the maximum anisotropy level in the full Pantheon sample is $AL_{max} = 0.361 \pm 0.070$ and corresponding direction $(l, b) = (123.05^{\circ} \pm 11.25^{\circ}, 4.78^{\circ} \pm 1.80^{\circ})$. A robust check shows the statistical significance of maximum anisotropy level is about 2.1σ . We also find that the Low- z and SNLS subsamples have decisive impact on the overall anisotropy while other three subsamples have little impact. Moreover, the anisotropy level map significantly rely on the inhomogeneous distribution of SNe Ia in the sky. For the DF method, we find the dipole anisotropy in the Pantheon sample is very weak. The dipole magnitude is constrained to be less than 1.16×10^{-3} at 95% confidence level. However, the dipole direction is well inferred by MCMC method and it points towards $(l, b) = (306.00^{\circ} \pm 82.95^{\circ}, -34.20^{\circ} \pm 16.82^{\circ})$. This direction is very close to the axial direction to the plane of SDSS subsample. It may imply that SDSS subsample is the decisive part to the dipole anisotropy in the full Pantheon sample. All these facts imply that the cosmic anisotropy found in Pantheon sample significantly rely on the inhomogeneous distribution of SNe Ia in the sky. More homogeneous distribution of SNe Ia is necessary to search for a more convincing cosmic anisotropy.

Key words: supernovae: general – large-scale structure of Universe

1 INTRODUCTION

The cosmological principle assumes that the Universe is homogeneous and isotropic at large scales. Based on it, the Λ CDM model is well consistent with current cosmological observations. For instance, the cosmic microwave background (CMB) radiation observed by the Wilkinson Microwave Anisotropy Probe (WMAP) (Bennett et al. 2013; Hinshaw et al. 2013) and Planck (Ade et al. 2016a,b) satellites confirm the Λ CDM model with high precision. However, the cosmological principle has been challenged by a lot of accurate observations. An incomplete list includes the hemispherical power asymmetry of CMB temperature anisotropies (Eriksen et al. 2004; Hansen et al. 2004; Bennett et al. 2013; Akrami et al. 2014; Ade et al. 2014; Quartin & Notari 2015), the alignment of low- ℓ multipoles in the CMB temperature anisotropies (Lineweaver et al. 1996; Tegmark et al. 2003; Bielewicz et al. 2004; Frommert & Enlin 2010; Copi et al. 2010), the parity asymmetry of low-

ℓ multipoles in angular power spectrum of CMB temperature anisotropies (Kim & Naselsky 2010a,b, 2011; Gruppuso et al. 2011; Zhao 2014), the large-scale alignment of quasar polarization vector (Hutsemekers & Lamy 2001; Hutsemekers et al. 2005). In addition, the spatial variation of fine-structure constant (Webb et al. 2011; King et al. 2012; Mariano & Perivolaropoulos 2012; Molaro et al. 2013) and MOND acceleration scale (Zhou et al. 2017; Chang et al. 2018b; Chang & Zhou 2019) are inconsistent with isotropic universe. These phenomena may imply a preferred direction of the Universe and hence a violation of the cosmological principle.

As standard candles, the supernovae of type Ia (SNe Ia) have been used to investigate the accelerating expansion of the Universe (Riess et al. 1998; Perlmutter et al. 1999), and the possible deviations from the isotropic universe (Schwarz & Weinhorst 2007; Gupta et al. 2008; Antoniou & Perivolaropoulos 2010; Blomqvist et al. 2010; Colin et al. 2011; Cai & Tuo 2012; Mariano & Perivolaropoulos 2012; Cai et al. 2013; Kalus et al. 2013; Zhao et al. 2013; Wang & Wang 2014; Yang et al. 2014; Chang et al. 2014a,b;

* Email: zhouyong@ihep.ac.cn

Heneka et al. 2014; Chang & Lin 2015; Bengaly et al. 2015; Li et al. 2015; Javanmardi et al. 2015; Lin et al. 2016a,b; Salehi & Aftabi 2016; Salehi & Setare 2017; Li & Lin 2017; Ghodsi et al. 2017; Wang & Wang 2018; Andrade et al. 2018b; Chang et al. 2018a; Deng & Wei 2018b), with the datasets given by the Union2 sample (Amanullah et al. 2010), the Union2.1 sample (Suzuki et al. 2012) and the “Joint Light-curve Analysis” (JLA) sample (Betoule et al. 2014). Antoniou & Perivolaropoulos (2010) first used the hemisphere comparison (HC) method to the Union2 sample and they found a certain cosmological preferred direction with maximum accelerating expansion rate. A similar preferred direction has been found in ω CDM and CPL parameterized model by Cai & Tuo (2012). Mariano & Perivolaropoulos (2012) first used the dipole fitting (DF) method to the Union2 sample and they found the existence of dark energy dipole at 2σ level. Zhao et al. (2013) used the Hierarchical Equal Area isoLatitude Pixelation¹ (HEALPix, Gorski et al. 2005) to divide the Union2 SNe Ia into 12 subsets and a dipole of deceleration parameter has been found at more than 2σ level. Meanwhile, a model-independent approach (Schwarz & Weinhorst 2007; Kalus et al. 2013) was used to estimate the cosmic anisotropy at low-redshift range. In addition, these works have been extended to include gamma-ray bursts (GRBs) (Wang & Wang 2014; Chang et al. 2014a) and the fine-structure constant (Mariano & Perivolaropoulos 2012; Li et al. 2015; Li & Lin 2017), and the preferred direction still exists. A similar cosmic anisotropy has been found in the Union2.1 sample (Yang et al. 2014; Javanmardi et al. 2015; Bengaly et al. 2015; Li et al. 2015; Lin et al. 2016b). Different with the Union2 or Union2.1 sample, the JLA sample doesn’t show any convincing evidence for the existence of the cosmic anisotropy (Bengaly et al. 2015; Lin et al. 2016a; Chang et al. 2018a; Wang & Wang 2018; Deng & Wei 2018b; Sun & Wang 2018a). Constraining the anisotropic amplitude and direction in Λ CDM, ω CDM and CPL models with the JLA sample gave a zero result (Lin et al. 2016a). No significant deviation from the isotropic universe was found through a redshift tomographic analysis on the JLA sample in the dipole-modulated Λ CDM model (Chang et al. 2018a). Constrained by the JLA sample, an anisotropic universe model with Bianchi-I metric was found to be consistent with the isotropic universe (Wang & Wang 2018). No significant dipole anisotropy (Deng & Wei 2018b; Sun & Wang 2018a) was found in JLA sample by using the CosmoMC (Lewis & Bridle 2002).

Recently, Scolnic et al. (2018) released the Pantheon sample which includes 1048 spectroscopically confirmed SNe Ia. The Pantheon sample comprises 279 SNe Ia discovered by the Pan-STARRS1 (PS1) Medium Deep Survey, and SNe Ia from various Low- z , SDSS, SNLS and HST surveys. The redshifts of these SNe Ia are in the range $0.01 < z < 2.26$. Compared to previous SNe Ia sample such as Union2 (Amanullah et al. 2010), Union2.1 (Suzuki et al. 2012) and JLA (Betoule et al. 2014), the number of SNe Ia in Pantheon sample is enlarged and all subsamples are cross-calibrated so that systematic uncertainties have been reduced. Therefore, the Pantheon sample is an ideal object to investigate the cosmic anisotropy. However, the cosmic anisotropy has

not been found in the Pantheon sample according to some researches (Andrade et al. 2018a; Deng & Wei 2018a; Sun & Wang 2018b; Li et al. 2019). Deng & Wei (2018a) employed the HC method, the DF method and HEALPix to the Pantheon sample, and they found null signal for the cosmic anisotropy. Sun & Wang (2018b) also used the HC method and DF method to the Pantheon sample, and they found the cosmic anisotropy is weakly dependent on redshift and the isotropic cosmological model is an excellent approximation. Meanwhile, Andrade et al. (2018a) used a model-independent analysis by selecting low-redshift subsamples, and they found the current SN Ia data favour the hypothesis of cosmic isotropy. In fact, the distribution of Pantheon SNe Ia is inhomogeneous in the sky, which could bring significant impact on the cosmic anisotropy. There are large distinctions between the distributions of each subsample, for example, the Low- z subsample is the most homogeneous while the PS1, SDSS and SNLS subsamples are extremely inhomogeneous in the sky. The distribution-dependence of methods that test the cosmic anisotropy has been noticed (Appleby & Shafieloo 2014; Chang & Lin 2015; Beltran Jimenez et al. 2015; Bengaly et al. 2015; Lin et al. 2016b; Andrade et al. 2018a; Sun & Wang 2018b). Chang & Lin (2015) and Lin et al. (2016b) suggested that the HC method strongly depends on the distribution of SNe Ia in the sky. Beltran Jimenez et al. (2015) found the preferred direction in the Union2 is aligned with the orthogonal direction of the SDSS observational plane. Bengaly et al. (2015) found that the dipolar direction of the Hubble map can be attributed to the intrinsic anisotropy of the JLA sample. It is worth investigating the impact of inhomogeneous distribution of Pantheon SNe Ia on the cosmic anisotropy.

As mentioned before, there are large distinctions between the distributions of each subsample. In order to investigate the impact of each subsample on the HC method and DF method, we will exclude individual subsamples from the Pantheon sample in turn. The full Pantheon sample and five combinations among Pantheon are used to test the cosmic anisotropy by performing the HC method and DF method, respectively. The rest of this paper is arranged as follows: In section 2, we introduce the Pantheon sample and its distribution in the sky. In section 3, we use the HC method to investigate the cosmic anisotropy. In section 4, we use the DF method to investigate the cosmic anisotropy. Finally, conclusions are given in section 5.

2 PANTHEON SAMPLE

Scolnic et al. (2018) compiled the Pantheon sample which includes 1048 spectroscopically confirmed SNe Ia. The Pantheon sample comprises 279 SNe Ia discovered by the Pan-STARRS1 (PS1) Medium Deep Survey, and SNe Ia from Low- z , SDSS, SNLS and HST subsamples, where Low- z is the compilation of all the smaller low- z surveys and HST is the compilation of all the HST surveys. The redshifts of these SNe Ia are in the range $0.01 < z < 2.26$. In Fig. 1, we display the distribution of these SNe Ia in the sky of the galactic coordinate system. As can be seen, the Pantheon SNe Ia are not uniformly distributed in the sky, half of them are located in the galactic south-east. The pseudo-colors indicate the redshift of these SNe Ia, which is also shown in

¹ <https://healpix.sourceforge.io/>

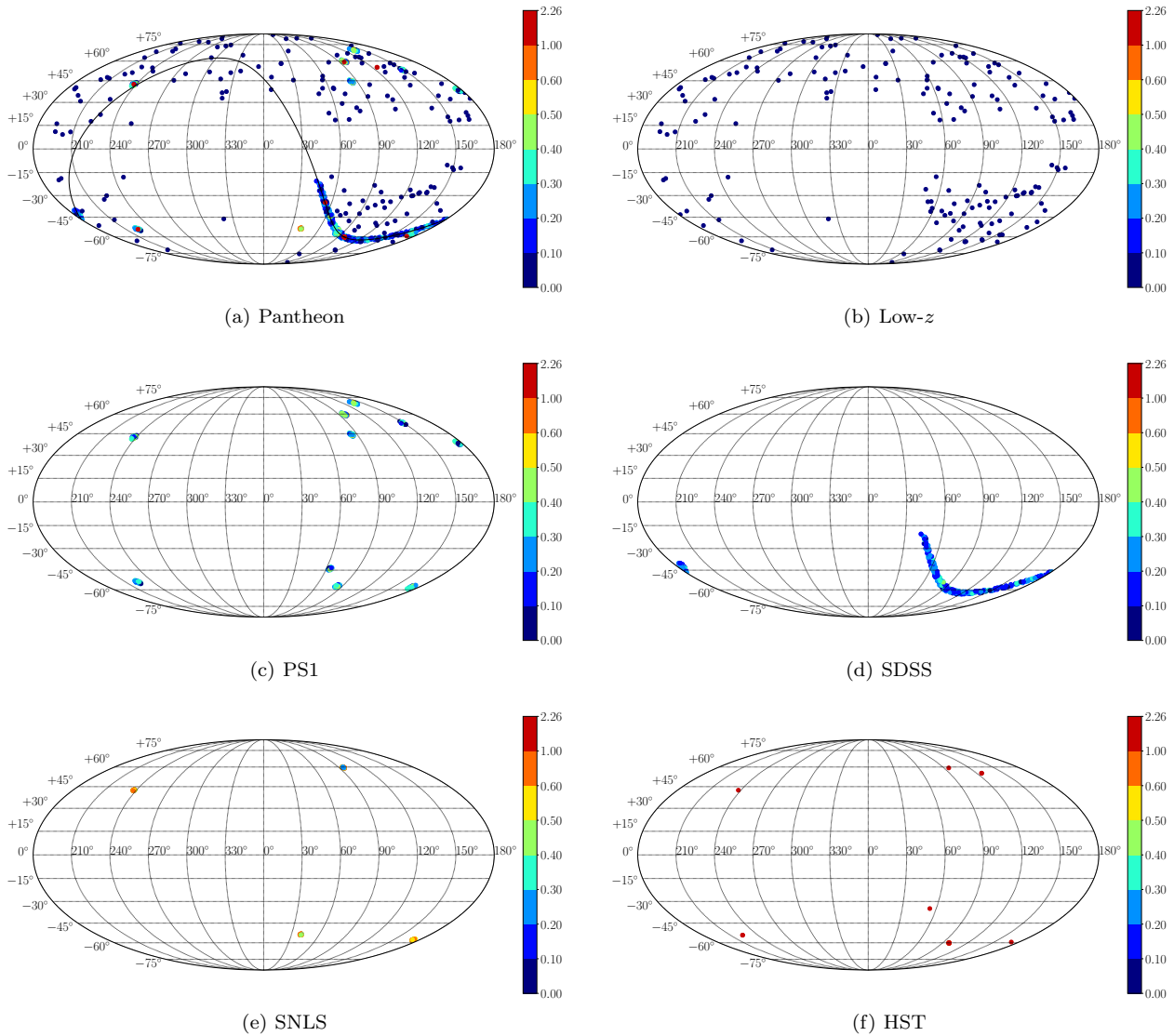


Figure 1. The distribution of 1048 Pantheon SNe Ia in the galactic coordinate system. The distribution of each subsample of Pantheon is also shown. The pseudo-colors represent the redshift of these SNe Ia. The black solid curve represents the celestial equator.

Fig. 2. Each subsample of Pantheon has different redshift range. We also display the sky distribution for each subsample of Pantheon in Fig. 1. It is found that three subsamples are extremely inhomogeneous in the sky. For the PS1 subsample, 279 SNe Ia cluster in ten directions, and each direction has nearly 30 SNe Ia. For the SDSS subsample, 335 SNe Ia cluster in a narrow strip which corresponds to the equator of the equatorial coordinate system. For the SNLS subsample, 236 SNe Ia cluster in four directions, and each direction has nearly 60 SNe Ia. Due to the cosmic anisotropy is sensitive to the spatial distribution, therefore these inhomogeneous distributions of SNe Ia could bring significant impact on the cosmic anisotropy. In this paper, we will employ the HC method and DF method to investigate the anisotropy of the Universe with the Pantheon sample. In order to investigate the impact of each subsample among Pantheon on the overall anisotropy, we exclude individual subsamples from the full Pantheon sample in turn. This method insures

enough SNe Ia used in our analysis. The full Pantheon sample and its five combinations are listed as follows,

- (1) Full Pantheon
- (2) Pantheon without Low- z
- (3) Pantheon without PS1
- (4) Pantheon without SDSS
- (5) Pantheon without SNLS
- (6) Pantheon without HST

Scolnic et al. (2018) employed the SALT2 (Guy et al. 2010) light-curve fitter to determine the observed distance modulus by using a modified version of the Tripp formula (Tripp 1998),

$$\mu_{obs} = m_B - M + \alpha x_1 - \beta c + \Delta_M + \Delta_B, \quad (1)$$

where μ_{obs} is the observed distance modulus, m_B is the apparent B -band magnitude and M is the absolute B -band magnitude of a fiducial SNe Ia with $x_1 = 0$ and $c = 0$. x_1 is the stretch parameter and α is the coefficient of the relation

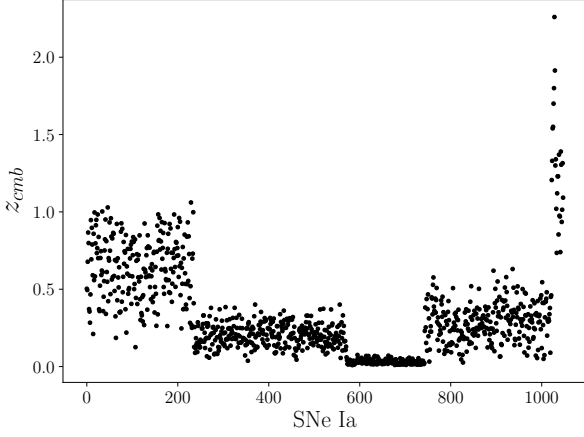


Figure 2. The redshift distributions of 1048 Pantheon SNe Ia. Each subsample of Pantheon has different redshift range. From left to right, the subsamples are SNLS, SDSS, Low- z , PS1 and HST.

between luminosity and stretch. c is the color parameter and β is the coefficient of the relation between luminosity and color. Δ_M is a distance correction based on the host galaxy mass of the SN and Δ_B is a distance correction based on predicted biases from simulations. Since the absolute magnitude of an SN Ia is degenerated with the Hubble constant, only the corrected apparent magnitudes are given in Scolnic et al. (2018), i.e. $m_{obs} = \mu_{obs} + M$. Then one can use these data to constrain the cosmological parameters.

In the standard cosmological model, the theoretical distance modulus takes the form,

$$\mu_{th} = 5 \log_{10} \frac{d_L}{\text{Mpc}} + 25, \quad (2)$$

where $d_L = (c/H_0)D_L$ is the luminosity distance, H_0 is the Hubble constant, c is the speed of light,

$$D_L = (1 + z_{hel}) \int_0^{z_{cmb}} \frac{dz}{E(z)}, \quad (3)$$

here z_{hel} is the heliocentric redshift and z_{cmb} is the CMB frame redshift. In the flat Λ CDM model, the dimensionless Hubble parameter is given as

$$E(z) = \sqrt{\Omega_m(1+z)^3 + (1-\Omega_m)}, \quad (4)$$

where Ω_m denotes the matter density at the present epoch. Then we can compare the observed apparent magnitude m_{obs} with the theoretical apparent magnitude m_{th} , and the latter is given as

$$m_{th} = \mu_{th} + M = 5 \log_{10} D_L + \mathcal{M}, \quad (5)$$

where the nuisance parameter \mathcal{M} depends on the absolute magnitudes M , and the Hubble constant H_0 .

To infer the best-fitting values of Ω_m and \mathcal{M} , we employ the χ^2 statistic,

$$\chi^2 = \Delta\boldsymbol{\mu}^T \cdot \mathbf{C}^{-1} \cdot \Delta\boldsymbol{\mu} = \Delta\mathbf{m}^T \cdot \mathbf{C}^{-1} \cdot \Delta\mathbf{m}, \quad (6)$$

where $\Delta\boldsymbol{\mu} = \boldsymbol{\mu}_{obs} - \boldsymbol{\mu}_{th}$ or $\Delta\mathbf{m} = \mathbf{m}_{obs} - \mathbf{m}_{th}$. The total covariance matrix \mathbf{C} is given as

$$\mathbf{C} = \mathbf{D}_{stat} + \mathbf{C}_{sys}, \quad (7)$$

where the diagonal matrix \mathbf{D}_{stat} represents the statistical

uncertainties and the covariance matrix \mathbf{C}_{sys} denotes systematic uncertainties. The best-fitting parameters can be obtained by minimizing χ^2 .

3 HEMISPHERE COMPARISON METHOD AND RESULT

The HC method has been widely used to investigate the cosmic anisotropy. For example, it has been used for investigating the anisotropic accelerating expansion of Universe (Schwarz & Weinhorst 2007; Antoniou & Perivolaropoulos 2010), the hemispherical power asymmetry of CMB temperature anisotropies (Ade et al. 2014; Akrami et al. 2014) and a varying MOND acceleration scale (Zhou et al. 2017). We can look for a preferred axis to describe the cosmic anisotropy by the HC method. The main steps of the HC method are as follows:

- (i) Generate an arbitrary direction $\hat{\mathbf{n}}(l, b)$ in the galactic coordinate system, where l and b are longitude and latitude, respectively. Divide the celestial sphere into “up” and “down” hemispheres according the direction $\hat{\mathbf{n}}$.
- (ii) Split the Pantheon dataset into two subsets according to the position of SNe Ia in the sky. One subset is located in “up” hemisphere and another subset is located in “down” hemisphere.
- (iii) Find the best-fitting value of Ω_m and its 1σ error on each hemisphere. Define the anisotropy level (AL) by the normalized difference as

$$\text{AL} \equiv \frac{\Delta\Omega_m}{\Omega_m} = 2 \cdot \frac{\Omega_{m,u} - \Omega_{m,d}}{\Omega_{m,u} + \Omega_{m,d}}. \quad (8)$$

The 1σ error of AL is given by

$$\sigma_{\text{AL}} = \frac{\sqrt{\sigma_{\Omega_{m,u}}^2 + \sigma_{\Omega_{m,d}}^2}}{\Omega_{m,u} + \Omega_{m,d}}. \quad (9)$$

- (iv) Repeat for adequate directions, find the maximum anisotropy level and its corresponding direction.

The HEALPix package (Gorski et al. 2005) is used to generate the directions (l, b) in the HC method with $N_{side} = 64$. The total number of the directions are $12 \times N_{side}^2 = 49152$, which is more denser than that in Deng & Wei (2018a) and Sun & Wang (2018b). The high resolution could benefit for us to find the maximum in the distribution of AL.

At first, we employ the HC method to investigate the cosmic anisotropy by using the full Pantheon sample. The anisotropy level map is shown in Fig. 3. The triangle marks the maximum anisotropy level in the sky. Note that the anisotropy level map in Fig. 3 is similar to Fig. 2 in Deng & Wei (2018a) and Fig. 2 in Sun & Wang (2018b), but high resolution used in this paper benefits for us to find the maximum anisotropy level. We find the maximum anisotropy level is $\text{AL}_{max} = 0.361 \pm 0.070$ and the corresponding direction is $(l, b) = (123.05^{+11.25^\circ}_{-4.22^\circ}, 4.78^{+1.80^\circ}_{-8.36^\circ})$. The 1σ range of the maximum anisotropy direction is identified by the direction that corresponds to an anisotropy level within 1σ from the maximum anisotropy level, i.e. $\text{AL} = \text{AL}_{max} \pm \sigma_{\text{AL}}$. In the preferred direction, the best-fitting values of Ω_m in “up” and “down” hemispheres are $\Omega_{m,u} = 0.313 \pm 0.023$ and

Table 1. The results of the HC method for the Pantheon sample and five combinations among Pantheon. We list the maximum AL and its corresponding direction (l, b) in the galactic coordinate system, and the best-fitting values of Ω_m in “up” and “down” hemispheres, as well as the total number N of SNe Ia and the number in each hemisphere.

Sample	N	N_u	N_d	$\Omega_{m,u}$	$\Omega_{m,d}$	AL_{max}	$l[^\circ]$	$b[^\circ]$
Full Pantheon	1048	883	165	0.313 ± 0.023	0.217 ± 0.029	0.361 ± 0.070	$123.05^{+11.25}_{-4.22}$	$4.78^{+1.80}_{-8.36}$
Pantheon without Low- z	876	456	420	0.361 ± 0.033	0.279 ± 0.027	0.257 ± 0.067	$98.44^{+37.27}_{-99.14}$	$26.61^{+17.59}_{-30.79}$
Pantheon without PS1	769	669	100	0.305 ± 0.024	0.199 ± 0.030	0.420 ± 0.076	$123.05^{+10.55}_{-4.92}$	$4.78^{+1.80}_{-7.77}$
Pantheon without SDSS	713	548	165	0.304 ± 0.025	0.217 ± 0.029	0.333 ± 0.073	$123.05^{+23.20}_{-36.56}$	$4.78^{+15.96}_{-28.75}$
Pantheon without SNLS	812	627	185	0.347 ± 0.031	0.215 ± 0.041	0.472 ± 0.092	$103.36^{+36.97}_{-35.16}$	$-28.63^{+35.21}_{-0.68}$
Pantheon without HST	1022	861	161	0.305 ± 0.024	0.214 ± 0.031	0.350 ± 0.076	$123.75^{+10.55}_{-2.81}$	$4.18^{+2.40}_{-7.76}$

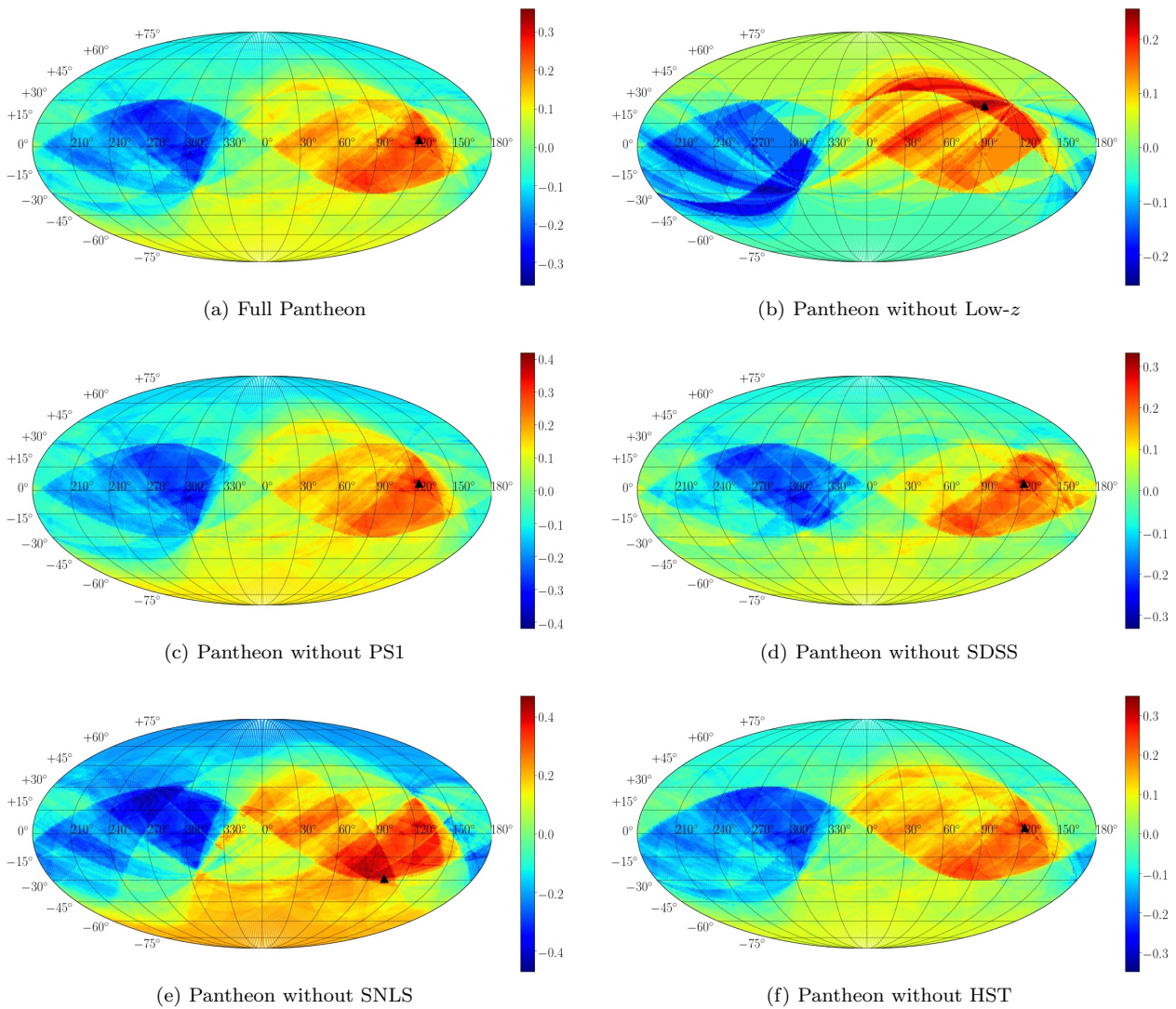


Figure 3. The pseudo-color map of the anisotropy level in the galactic coordinate system, derived from the HC method to the full Pantheon sample and five combinations among Pantheon. The triangle marks the maximum anisotropy level in the sky.

$\Omega_{m,d} = 0.217 \pm 0.029$, respectively. Since the deceleration parameter $q_0 = -1 + 3\Omega_m/2$ in the flat Λ CDM model, the minimum accelerating expansion of Universe is in the direction of maximum AL, while the maximum accelerating expansion is in the opposite direction. However, we find the numbers of SNe Ia in “up” and “down” hemispheres are 883 and 165,

respectively. The hemispheric asymmetry of Pantheon SNe Ia is shown in Fig. 4. The inhomogeneous distribution of Pantheon SNe Ia in the sky could have significant impact on the anisotropy level in HC method. We will discuss this issue later. All related results are summarized in Table 1. In addition, we also perform the HC method for the nuisance

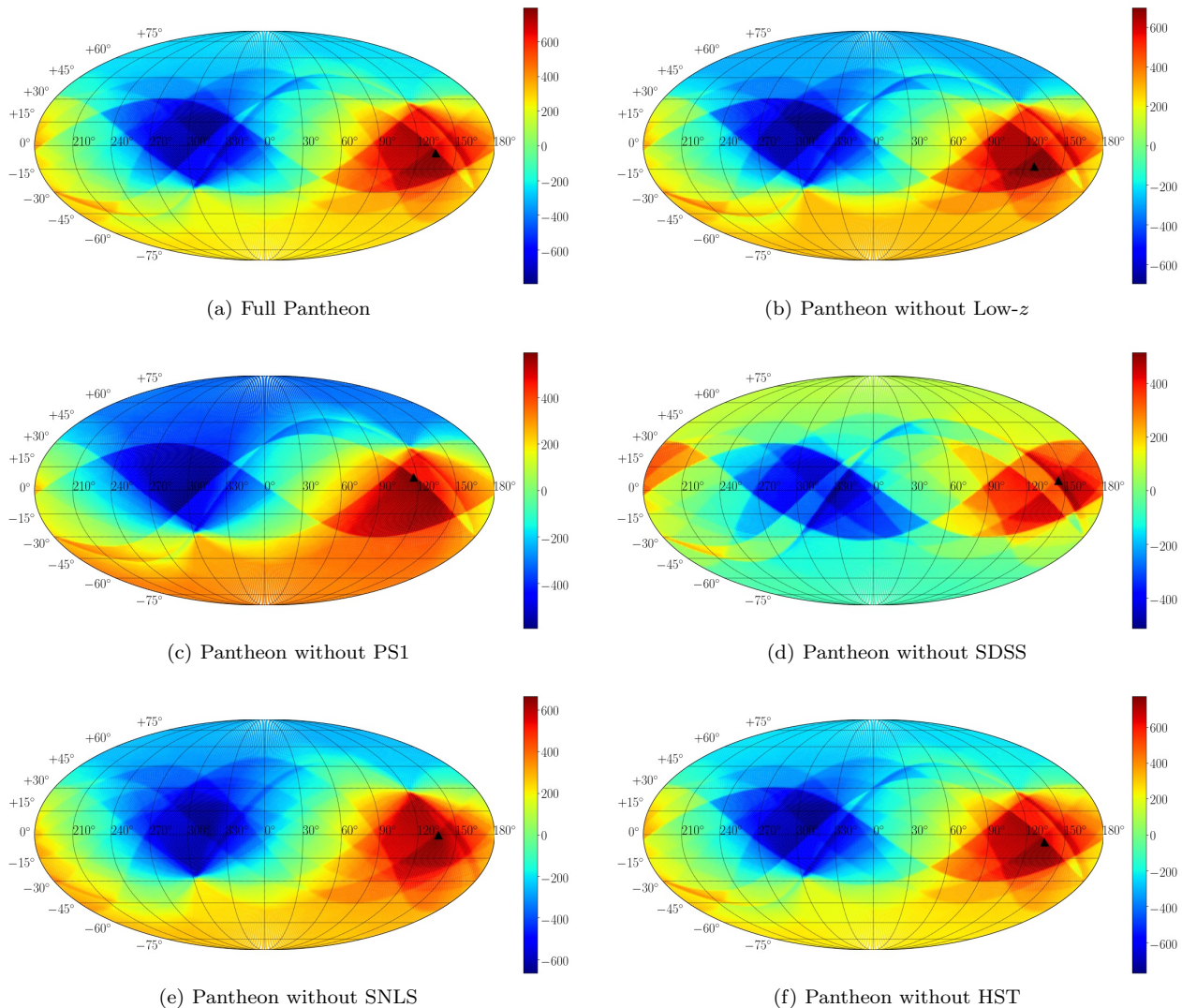


Figure 4. The pseudo-color map of AL_N in the galactic coordinate system for the full Pantheon sample and five combinations among Pantheon. The triangle marks the maximum number difference in the sky.

parameter \mathcal{M} . We find its maximum anisotropy level is less than 0.3%, showing that no obvious signal of anisotropy was found for \mathcal{M} with the Pantheon sample.

As a robust check, it is necessary to examine whether the maximum anisotropy level from the full Pantheon sample is consistent with statistical isotropy. The simulated isotropic data set is constructed by replacing the i th observed apparent magnitude $m_{obs,i}$ of the Pantheon sample by a random number from a Gaussian distribution with the mean determined by Eq. (5), where $\Omega_m = 0.298$, $\mathcal{M} = 23.809$ is the best fitting value to the full Pantheon sample, and the standard deviation is equal to the statistical uncertainty of $m_{obs,i}$. Then one can employ the HC method to this simulated isotropic data set and compare the maximum anisotropy level with that derived from the full Pantheon sample. Given the limitations of computing time, we construct 200 simulated isotropic data sets and they have acceptable statistics. The maximum anisotropy level from the HC method to these data sets is shown in Fig. 5. The distribution is fitted by a Gaussian function, the mean value is

0.251 and the standard deviation is 0.053. As can be seen, the maximum anisotropy level from the full Pantheon sample is hardly reproduced by simulated isotropic data set and its statistical significance is about 2.1σ .

In order to investigate the impact of each subsample among Pantheon on the overall anisotropy in the full Pantheon, we exclude individual subsamples from the full Pantheon sample in turn and five combinations among Pantheon are used, which are listed in Sec. 2. We employ the HC method to these five combinations. The anisotropy level map for each combination is shown in Fig. 3 and all related results are summarized in Table 1. As can be seen, the AL map of the Pantheon without Low- z or SNLS subsample has obvious difference with the AL map of the full Pantheon sample while other three combinations are consistent with the full Pantheon. It may imply that the Low- z and SNLS subsamples have significant impact on the overall anisotropy in the full Pantheon. For the Pantheon without SNLS subsample, we find that the maximum anisotropy level is $AL_{max} = 0.472 \pm 0.092$ and the corresponding di-

Table 2. The maximum number difference and the number of SNe Ia in “up” and “down” hemisphere, and the corresponding direction for the full Pantheon sample and five combinations among Pantheon.

Sample	AL_N	N_u	N_d	$l[^\circ]$	$b[^\circ]$
Full Pantheon	796	922	126	133.95	-4.48
Pantheon without Low- z	700	788	88	127.85	-13.01
Pantheon without PS1	595	682	87	117.07	8.39
Pantheon without SDSS	515	614	99	145.20	6.28
Pantheon without SNLS	666	739	73	135.70	0
Pantheon without HST	772	897	125	133.95	-4.48

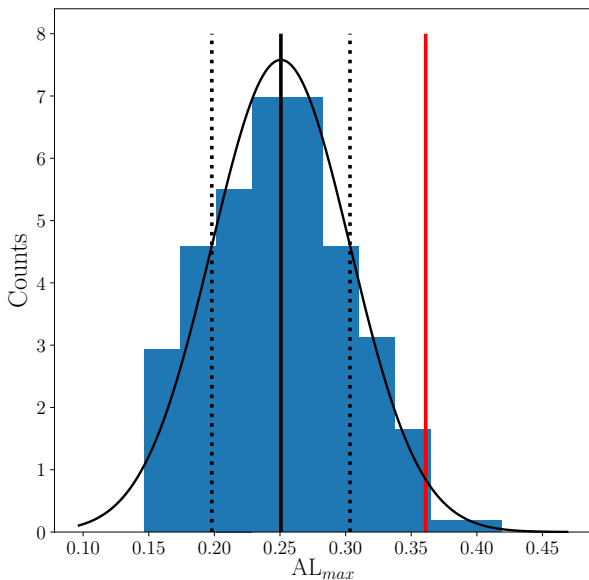


Figure 5. The distribution of the maximum anisotropy level in 200 simulated isotropic data sets, with black curve the best-fitting result to Gaussian function. Note that the counts have been normalized. The black solid and dashed vertical lines show the mean and the standard deviation, respectively. The red vertical line shows the maximum anisotropy level from the full Pantheon sample.

rection is $(l, b) = (103.36^{+37.97^\circ}_{-35.16^\circ}, -28.63^{+35.21^\circ}_{-0.68^\circ})$. This direction is 38.41° away from the preferred direction in the full Pantheon. For the Pantheon without Low- z subsample, we find that the maximum anisotropy level is $AL_{max} = 0.257 \pm 0.067$ and the corresponding direction is $(l, b) = (98.44^{+37.27^\circ}_{-99.14^\circ}, 26.61^{+17.59^\circ}_{-30.79^\circ})$. This direction is 32.07° away from the preferred direction in the full Pantheon. Moreover, we employ the HC method to the combination of Low- z and SNLS subsamples. We find a consistent preferred direction with that in the full Pantheon sample. The AL map is shown in Fig. 6. The maximum anisotropy level is $AL_{max} = 0.342 \pm 0.090$ and the corresponding direction is $(l, b) = (123.05^{+11.25^\circ}_{-4.92^\circ}, 4.78^{+1.80^\circ}_{-8.36^\circ})$. These results confirm that the anisotropy in the full Pantheon sample is mostly originating from the Low- z and SNLS subsamples.

For the full Pantheon sample and the combinations among Pantheon, we find the numbers of SNe Ia in “up” and “down” hemispheres have big difference in the maximum

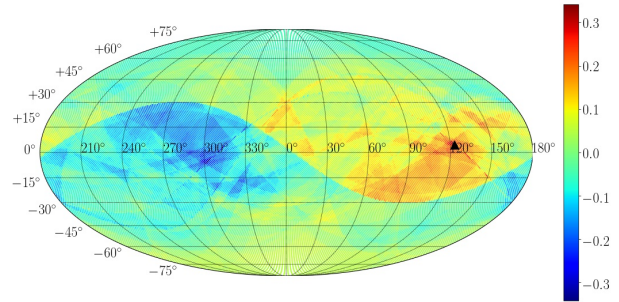


Figure 6. The pseudo-color map of the anisotropy level in the galactic coordinate system, derived from the HC method to the combination of Low- z and SNLS subsamples. The triangle marks the maximum anisotropy level in the sky.

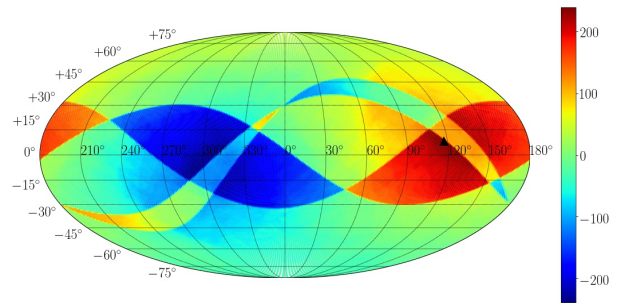


Figure 7. The pseudo-color map of AL_N in the galactic coordinate system for the combination of Low- z and SNLS subsamples. The triangle marks the maximum number difference in the sky.

anisotropy direction. In order to investigate the possible relation between the anisotropy level with the inhomogeneous distribution of SNe Ia in the galactic coordinate system, we define the number difference $AL_N = N_u - N_d$ between the numbers of SNe Ia in “up” and “down” hemispheres, respectively. The distributions of AL_N for the full Pantheon sample and five combinations among Pantheon are shown in Fig. 4. The maximum AL_N and the corresponding directions are listed in Table 2. For the full Pantheon sample, the direction of the maximum AL_N is $(l, b) = (133.95^\circ, -4.48^\circ)$, and there are 922 SNe Ia in “up” hemisphere while only 126 SNe Ia in “down” hemisphere. In this direction, there are much more SNe Ia in “up” hemisphere than that in “down” hemisphere for each subsample. Even though individual subsamples have been excluded from the full Pantheon sample, there still be much more SNe Ia in the same “up” hemisphere due to the contributions of other four subsamples. This may be the reason why the direction of maximum AL_N in each combination is close to the direction in the full Pantheon. For the Pantheon without Low- z (SNLS) subsample, the direction of maximum AL_N is only 10.44° (4.81°) away from that in the full Pantheon. It is interesting to note that the maximum anisotropy direction in full Pantheon is close to the direction of the maximum AL_N and its angle difference is only 14.29° . In addition, the distribution of AL_N for the combination of Low- z and SNLS subsamples is shown in Fig. 7. The direction of the maximum AL_N is $(l, b) = (117.07^\circ, 8.39^\circ)$, which is 6.95° away from the maximum anisotropy direction for the same combination. It may

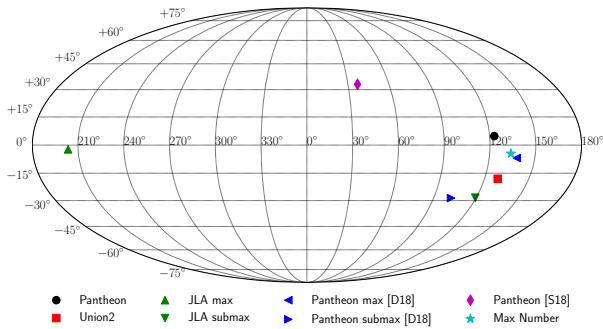


Figure 8. The HC preferred direction from the Pantheon sample and that from the Union2 sample (Antoniou & Perivolaropoulos 2010), the JLA sample (Deng & Wei 2018b) and the Pantheon sample (Deng & Wei 2018a; Sun & Wang 2018b). The star marks the direction of the maximum number difference in the full Pantheon sample.

imply that the anisotropy level of the Pantheon sample significantly rely on the inhomogeneous distribution of SNe Ia in the sky.

At the end of this section, we make some comparisons between the HC preferred direction in the Pantheon sample with that derived from the Union2 sample (Antoniou & Perivolaropoulos 2010), the JLA sample (Deng & Wei 2018b) and the Pantheon sample (Deng & Wei 2018a; Sun & Wang 2018b). The HC preferred direction in each SNe Ia sample is shown in Fig. 8, in the galactic coordinate system. As mentioned before, we find a similar anisotropy level map in the Pantheon sample with that in Deng & Wei (2018a) and Sun & Wang (2018b), but high resolution benefit for us to find the maximum anisotropy level. In Deng & Wei (2018a), the maximum anisotropy level is $AL_{max} = 0.3088 \pm 0.0738$ and the corresponding direction $(l, b) = (138.08^{+3.16}_{-16.90}, -6.84^{+13.55}_{-2.31})$, which is consistent with the preferred direction in this paper within 1σ error. However, the maximum anisotropy level in Sun & Wang (2018b) is $AL_{max} = 0.136^{+0.009}_{-0.005}$, much less than 0.361 and the corresponding direction $(l, b) = (37^\circ \pm 40^\circ, 33^\circ \pm 16^\circ)$ totally deviates from the preferred direction in this paper, which could mean the 500 axes used in their work are not enough. The maximum anisotropy direction in the JLA sample (Deng & Wei 2018b) is not consistent with that in this paper, but the submaximum anisotropy direction $(l, b) = (119.47^{+46.13}_{-23.39}, -28.39^{+17.01}_{-6.52})$ is about 33.35° away from the preferred direction in this paper. Interestingly, in the Union2 sample (Antoniou & Perivolaropoulos 2010), the maximum anisotropy level is $AL_{max} = 0.43 \pm 0.06$ and the corresponding direction $(l, b) = (129^{+23}_{-3}, -18^{+10}_{-11})$ is 23.52° away from the preferred direction in the Pantheon sample. In addition, we find these HC preferred directions from different SNe Ia samples are close to the direction of the maximum number difference in the full Pantheon. The consistency confirms the conclusion that the HC method strongly depends on the distribution of SNe Ia in the sky (Chang & Lin 2015; Lin et al. 2016b).

4 DIPOLE FITTING METHOD AND RESULT

The DF method was first employed to analyse the cosmic anisotropy using the Union2 SNe Ia sample (Mariano & Perivolaropoulos 2012). Then, it has been widely used for the spatial variation of fine structure (Webb et al. 2011; King et al. 2012) and MOND acceleration scale (Chang et al. 2018b). We consider an expression of the theoretical apparent magnitude with monopole and dipole correction, namely

$$\tilde{m}_{th} = m_{th}[1 + A + B(\hat{n} \cdot \hat{p})], \quad (10)$$

where \hat{n} is the dipole direction in the sky and \hat{p} is the unit vector pointing to the position of SNe Ia. A and B represent the monopole term and dipole magnitude, respectively. m_{th} is the fiducial theoretical apparent magnitude predicted by the flat Λ CDM model given by Eq. (5). In galactic coordinate system, the dipole direction can be represented by

$$\hat{n} = \cos(l) \cos(b) \hat{i} + \sin(l) \cos(b) \hat{j} + \sin(b) \hat{k}, \quad (11)$$

where l and b are the galactic longitude and latitude, respectively. \hat{i} , \hat{j} and \hat{k} are unit vectors along the axis in the Cartesian coordinates system. Similarly, the position of the i th SNe Ia can be represented by

$$\hat{p}_i = \cos(l_i) \cos(b_i) \hat{i} + \sin(l_i) \cos(b_i) \hat{j} + \sin(b_i) \hat{k}. \quad (12)$$

Two parameters (Ω_m, \mathcal{M}) are used to predict the fiducial theoretical apparent magnitude. Four parameters (A, B, l, b) are used to describe the dipole anisotropy of the Universe. In total, there are six parameters used in the DF method. The best-fitting parameters can be derived by minimizing the corresponding χ^2 . We implement the Bayesian analysis to infer the best-fitting parameters and their 1σ error, by using the affine-invariant Markov chain Monte Carlo (MCMC) ensemble sampler in *emcee*¹ (Foreman-Mackey et al. 2013), which is widely used in astrophysics and cosmology. In Bayesian analysis, the posterior distributions are determined by priors and likelihood functions, the latter is $\mathcal{L} \propto \exp(-\chi^2/2)$. The *emcee* could be regarded as a supplement of the CosmoMC (Lewis & Bridle 2002). In this paper, one hundred random walkers are used to explore the entire parameter space. We run 500 iterations in the burn-in phase and another 2000 iterations in the production phase, which is sufficient for this analysis. We check that the acceptance fractions for all random walkers are in the range (0.2, 0.5). The flat prior on each parameter is used as follow: $\Omega_m \sim [0, 1]$, $\mathcal{M} \sim [0, 100]$, $A \sim [-1, 1]$, $B \sim [0, 1]$, $l \sim [-180, 180]^\circ$, $b \sim [-90^\circ, 90^\circ]$.

At first, we employ the DF method to investigate the cosmic anisotropy by using the full Pantheon sample. The marginalized posterior distributions of the DF method are shown in Fig. 9. We find the dipole anisotropy in the full Pantheon sample is very weak. The maximum of monopole term A and the dipole magnitude B are well consistent with zero within 1σ . The monopole term is $A = (1.91^{+7.80}_{-6.25}) \times 10^{-3}$, and the dipole magnitude is less than 1.16×10^{-3} at 95% confidence level (CL). This result is consistent with that in Deng & Wei (2018a) at the same magnitude. Benefiting from the usage of *emcee*, we obtain the detailed posterior distribution on the dipole direction. Fig. 9 shows that the dipole direction is $(l, b) = (306.00^{+82.95}_{-125.01}, -34.20^{+16.82}_{-54.93})$,

¹ <https://emcee.readthedocs.io/en/stable/>

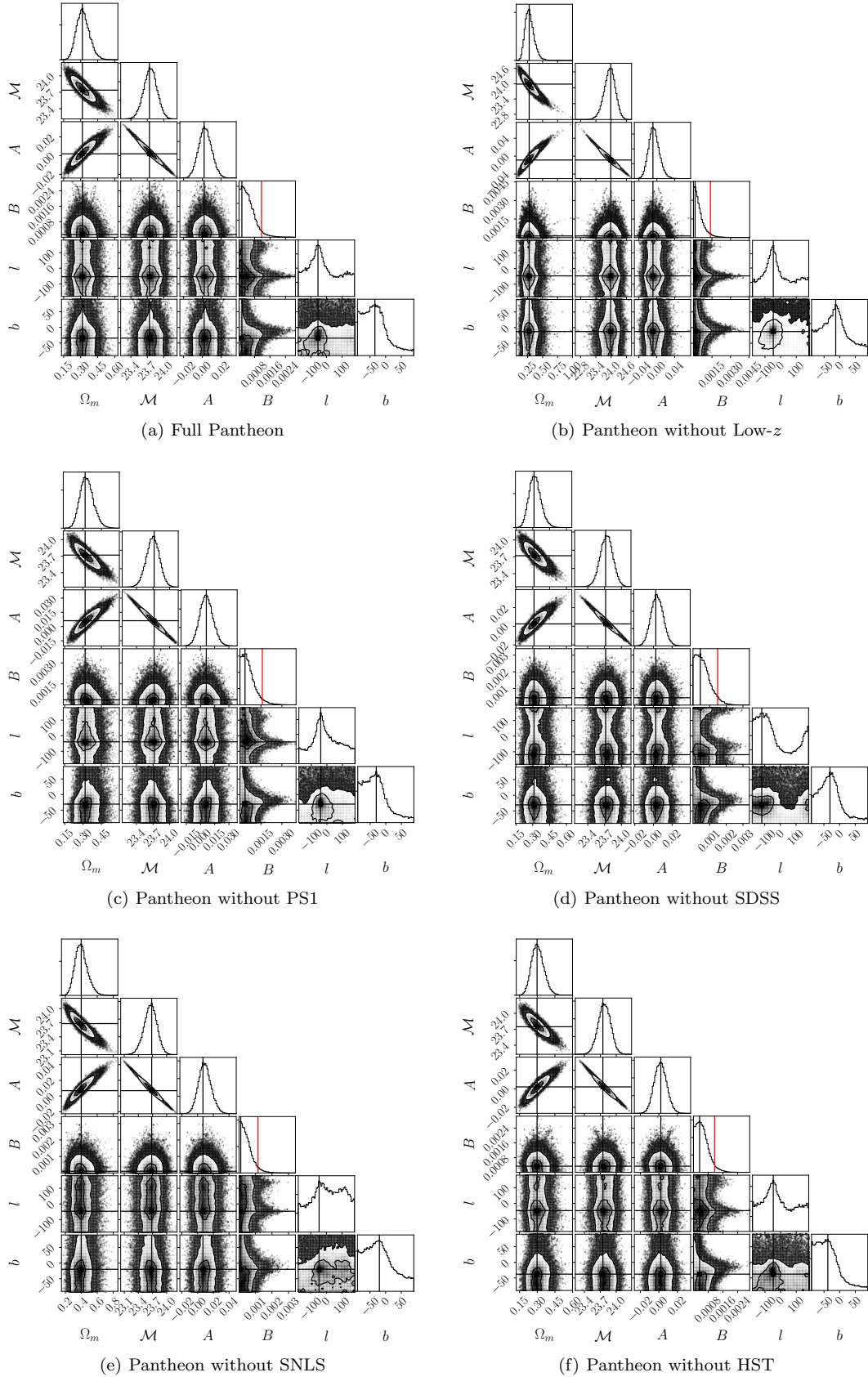
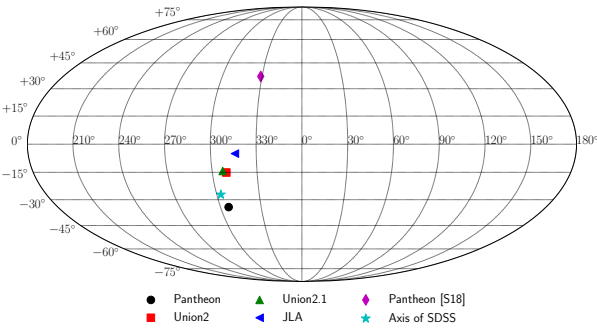


Figure 9. The 1-dimensional and 2-dimensional marginalized posterior distributions by using the DF method to the full Pantheon sample and five combinations among Pantheon. The horizontal and vertical solid black lines mark the maximum of 1-dimensional marginalized posteriors. The red line indicates the 95% CL upper limit of dipole magnitude B .

Table 3. The results of the DF method for the full Pantheon sample and five combinations among Pantheon. We show the maximum and its 68% CL constraints on the model parameters Ω_m , \mathcal{M} , A , l and b , the 95% CL upper limits of dipole magnitude B in each combination.

Sample	N	Ω_m	\mathcal{M}	$A[10^{-3}]$	$B[10^{-3}]$	$l[^\circ]$	$b[^\circ]$
Full Pantheon	1048	$0.315^{+0.059}_{-0.054}$	$23.739^{+0.140}_{-0.102}$	$1.91^{+7.80}_{-6.25}$	< 1.16	$306.00^{+82.95}_{-125.01}$	$-34.20^{+16.82}_{-54.93}$
Pantheon without Low- z	876	$0.276^{+0.068}_{-0.075}$	$23.985^{+0.185}_{-0.254}$	$-8.64^{+12.93}_{-10.54}$	< 1.37	$313.20^{+99.18}_{-101.58}$	$-12.60^{+28.55}_{-58.98}$
Pantheon without PS1	769	$0.317^{+0.062}_{-0.047}$	$23.720^{+0.142}_{-0.131}$	$6.14^{+6.44}_{-7.37}$	< 1.60	$320.40^{+135.85}_{-57.75}$	$-30.61^{+12.42}_{-58.90}$
Pantheon without SDSS	713	$0.311^{+0.056}_{-0.049}$	$23.719^{+0.131}_{-0.095}$	$2.50^{+7.89}_{-5.24}$	< 1.48	$241.21^{+76.31}_{-84.08}$	$-30.60^{+24.15}_{-44.62}$
Pantheon without SNLS	812	$0.399^{+0.070}_{-0.082}$	$23.682^{+0.121}_{-0.150}$	$6.85^{+9.46}_{-6.65}$	< 1.15	$313.19^{+188.66}_{-27.58}$	$-19.80^{+20.14}_{-69.04}$
Pantheon without HST	1022	$0.298^{+0.050}_{-0.054}$	$23.748^{+0.142}_{-0.092}$	$2.08^{+5.90}_{-7.50}$	< 1.15	$313.21^{+83.15}_{-133.00}$	$-37.80^{+12.76}_{-52.11}$

**Figure 10.** The dipole direction from the Pantheon sample and that from the Union2 sample (Mariano & Perivolaropoulos 2012), the Union2.1 sample (Yang et al. 2014), the JLA sample (Lin et al. 2016a) and the Pantheon sample (Sun & Wang 2018b). The star marks the axial direction to the plane of SDSS subsample.

here the galactic longitude is converted to positive value. The very large uncertainty of dipole direction also implies that the dipole anisotropy in the Pantheon sample is very weak. On the other hand, the maximum of Ω_m and \mathcal{M} are almost the same as that without dipole anisotropy. The related results of the DF method are listed in Table 3.

As same as the HC method, we employ the DF method to those five combinations among Pantheon. The marginalized posterior distribution for each combination is shown in Fig. 9 and all related results are summarized in Table 3. We find the dipole anisotropy in each combination is also very weak. The dipole direction is consistent with that in the full Pantheon sample, except one combination has large deviation. For the Pantheon without SDSS subsample, the dipole direction is $(l, b) = (241.21^{+76.31^\circ}_{-84.08^\circ}, -30.60^{+24.15^\circ}_{-44.62^\circ})$, about 53.89° away from the dipole direction in full Pantheon. Note that there are 335 SNe Ia in the SDSS subsample clustering in a narrow strip which corresponds to the equator of the equatorial coordinate system. Coincidentally, the axial direction of equator with galactic coordinates $(l, b) = (302.93^\circ, -27.13^\circ)$ is very close to the dipole direction in the full Pantheon sample and its angle difference is only 7.55° . Therefore, the SDSS subsample could be the decisive part that impacts the dipole anisotropy in the full Pantheon sample. Similar conclusions have been found in the Union2 sample (Beltran Jimenez et al. 2015).

At the end, we make some comparisons between the dipole direction in the Pantheon sample with that derived from the Union2 sample (Mariano & Perivolaropoulos 2012),

the Union2.1 sample (Yang et al. 2014), the JLA sample (Lin et al. 2016a) and the Pantheon sample (Sun & Wang 2018b). The dipole direction in each SNe Ia sample are shown in Fig. 10, in the galactic coordinate system. As we can see, the dipole direction in Sun & Wang (2018b) is $(l, b) = (329^{+101^\circ}_{-28^\circ}, 37^{+52^\circ}_{-21^\circ})$, totally deviates from all other dipole directions. Even though the dipole direction in JLA sample (Lin et al. 2016a) is $(l, b) = (316^{+107^\circ}_{-110^\circ}, -5^{+41^\circ}_{-60^\circ})$, about 30.64° away from the dipole directions in the full Pantheon sample. However, we find the dipole direction in Pantheon and JLA sample are close to the dipole direction in the Union2 or Union2.1 sample (Mariano & Perivolaropoulos 2012; Yang et al. 2014). All of these dipole directions are close to each other hinting that there could exist an underlying relation. The star in Fig. 10 indicates the axial direction to the plane of SDSS subsample, which is well close to these dipole directions, especially for the dipole direction in the Pantheon sample. Since the large deviation for the Pantheon without SDSS subsample, it may imply that the dipole anisotropy in the Pantheon sample is mostly determined by the distribution of the SDSS subsample, and other subsamples only have small impact.

5 CONCLUSIONS

The cosmological principle has been extensively tested by SNe Ia and the cosmic anisotropy is preferred by most observations. However, the distribution of SNe Ia is very inhomogeneous in the sky, which could bring significant impact on the cosmic anisotropy. In this paper, we employed the hemisphere comparison (HC) method and the dipole fitting (DF) method to investigate the cosmic anisotropy in the full Pantheon sample as well as five combinations among Pantheon. The combinations are obtained by excluding individual subsamples from the Pantheon sample in turn.

For the HC method, we found the anisotropy level map of the full Pantheon sample is similar to the results in Deng & Wei (2018a) and Sun & Wang (2018b). Benefiting from the usage of HEALPix, we found the maximum anisotropy level is $AL_{max} = 0.361 \pm 0.070$ and corresponding direction is $(l, b) = (123.05^{+11.25^\circ}_{-4.22^\circ}, 4.78^{+1.80^\circ}_{-8.36^\circ})$. In this direction, the Universe has the minimum accelerating expansion while the maximum one is in the opposite direction. As a robust check, we found the maximum anisotropy level from the full Pantheon sample is hardly reproduced by simulated isotropic data set and its statistical significance is about 2.1σ . The numbers of SNe Ia in “up” and “down” hemispheres are

883 and 165, respectively. The inhomogeneous distribution of Pantheon SNe Ia in the sky could have significant impact on the anisotropy level in HC method. According to the anisotropy level map in Fig. 3, we found that the HC preferred direction in the Pantheon without Low- z or SNLS subsample has large deviation from the HC preferred direction in the full Pantheon sample. We also employed the HC method to the combination of Low- z and SNLS subsamples. We found a consistent preferred direction with that in the full Pantheon sample. All of these results show the Low- z and SNLS subsamples have decisive impact on the HC result of the full Pantheon sample. In addition, we found the direction of the maximum number difference is close to the maximum anisotropy direction for the full Pantheon sample and the combination of low- z and SNLS subsample. It may imply that the anisotropy level of the Pantheon sample significantly rely on the inhomogeneous distribution of SNe Ia in the sky. At the end, we made some comparisons with the HC preferred direction in the Union2 sample (Antoniu & Perivolaropoulos 2010), the JLA sample (Deng & Wei 2018b) and the Pantheon sample (Deng & Wei 2018a; Sun & Wang 2018b). Interestingly, we found the preferred direction in the Pantheon sample is close to that in the Union2 sample, and its angle difference is only 23.52° . The consistency confirms the conclusion that the HC method strongly depends on the distribution of SNe Ia in the sky (Chang & Lin 2015; Lin et al. 2016b).

For the DF method, we implemented the Bayesian analysis by using the MCMC method to infer the best-fitting parameters and their 1σ error. According to the marginalized posterior distributions in Fig. 9, we found the dipole anisotropy in the Pantheon sample is very weak. The monopole term and the dipole magnitude are well consistent with zero within 1σ . The monopole term is $A = (1.91_{-6.25}^{+7.80}) \times 10^{-3}$, and the dipole magnitude is less than 1.16×10^{-3} at 95% CL. However, the dipole direction is well inferred by MCMC method and it points towards $(l, b) = (306.00^\circ_{-125.01^\circ}^{+82.95^\circ}, -34.20^\circ_{-54.93^\circ}^{+16.82^\circ})$. The DF method was also employed to each combination among Pantheon. We found the dipole direction in the Pantheon without SDSS subsample has a large deviation, about 53.89° away from the dipole direction in the full Pantheon sample. In addition, the axial direction to the plane of SDSS subsample is very close to the dipole direction in the full Pantheon and its angle difference is only 7.55° . It implies that the SDSS subsample could be the decisive part that impacts the dipole anisotropy in the full Pantheon sample. We also found the dipole direction in the Union2 sample is close to that in the Pantheon sample, and the SDSS subsample could also be the decisive part to the dipole anisotropy in Union2 sample.

All of these results imply that the cosmic anisotropy found in Pantheon sample significantly rely on the inhomogeneous distribution of SNe Ia in the sky. More homogeneous distribution of SNe Ia is necessary to search for a convincing cosmic anisotropy.

ACKNOWLEDGEMENTS

We thank the anonymous referee for valuable suggestions and comments. We appreciate Dr. Y. Sang for useful discussions. This work has been funded by the National Natural

Science Foundation of China under Grant Nos. 11675182 and 11690022.

References

- Ade P. A. R., et al., 2014, *Astron. Astrophys.*, 571, A23
 Ade P. A. R., et al., 2016a, *Astron. Astrophys.*, 594, A13
 Ade P. A. R., et al., 2016b, *Astron. Astrophys.*, 594, A20
 Akrami Y., Fantaye Y., Shafieloo A., Eriksen H. K., Hansen F. K., Banday A. J., Grski K. M., 2014, *Astrophys. J.*, 784, L42
 Amanullah R., et al., 2010, *Astrophys. J.*, 716, 712
 Andrade U., Bengaly C. A. P., Santos B., Alcaniz J. S., 2018a, *Astrophys. J.*, 865, 119
 Andrade U., Bengaly C. A. P., Alcaniz J. S., Santos B., 2018b, *Phys. Rev.*, D97, 083518
 Antoniu I., Perivolaropoulos L., 2010, *JCAP*, 1012, 012
 Appleby S., Shafieloo A., 2014, *JCAP*, 1403, 007
 Beltran Jimenez J., Salzano V., Lazkoz R., 2015, *Phys. Lett.*, B741, 168
 Bengaly C. A. P., Bernui A., Alcaniz J. S., 2015, *Astrophys. J.*, 808, 39
 Bennett C. L., et al., 2013, *Astrophys. J. Suppl.*, 208, 20
 Betoule M., et al., 2014, *Astron. Astrophys.*, 568, A22
 Bielewicz P., Gorski K. M., Banday A. J., 2004, *Mon. Not. Roy. Astron. Soc.*, 355, 1283
 Blomqvist M., Enander J., Mortsell E., 2010, *JCAP*, 1010, 018
 Cai R.-G., Tuo Z.-L., 2012, *JCAP*, 1202, 004
 Cai R.-G., Ma Y.-Z., Tang B., Tuo Z.-L., 2013, *Phys. Rev.*, D87, 123522
 Chang Z., Lin H.-N., 2015, *Mon. Not. Roy. Astron. Soc.*, 446, 2952
 Chang Z., Zhou Y., 2019, *Mon. Not. Roy. Astron. Soc.*, 486, 1658
 Chang Z., Li X., Lin H.-N., Wang S., 2014a, *Mod. Phys. Lett.*, A29, 1450067
 Chang Z., Li X., Lin H.-N., Wang S., 2014b, *Eur. Phys. J.*, C74, 2821
 Chang Z., Lin H.-N., Sang Y., Wang S., 2018a, *Mon. Not. Roy. Astron. Soc.*, 478, 3633
 Chang Z., Lin H.-N., Zhao Z.-C., Zhou Y., 2018b, *Chin. Phys.*, C42, 115103
 Colin J., Mohayaee R., Sarkar S., Shafieloo A., 2011, *Mon. Not. Roy. Astron. Soc.*, 414, 264
 Copi C. J., Huterer D., Schwarz D. J., Starkman G. D., 2010, *Adv. Astron.*, 2010, 847541
 Deng H.-K., Wei H., 2018a, *Eur. Phys. J.*, C78, 755
 Deng H.-K., Wei H., 2018b, *Phys. Rev.*, D97, 123515
 Eriksen H. K., Hansen F. K., Banday A. J., Gorski K. M., Lilje P. B., 2004, *Astrophys. J.*, 605, 14
 Foreman-Mackey D., Hogg D. W., Lang D., Goodman J., 2013, *Publ. Astron. Soc. Pac.*, 125, 306
 Frommert M., Enlin T. A., 2010, *Mon. Not. Roy. Astron. Soc.*, 403, 1739
 Ghodsi H., Baghran S., Habibi F., 2017, *JCAP*, 1710, 017
 Gorski K. M., Hivon E., Banday A. J., Wandelt B. D., Hansen F. K., Reinecke M., Bartelman M., 2005, *Astrophys. J.*, 622, 759
 Gruppuso A., Finelli F., Natoli P., Paci F., Cabella P.,

- De Rosa A., Mandolesi N., 2011, *Mon. Not. Roy. Astron. Soc.*, 411, 1445
- Gupta S., Saini T. D., Laskar T., 2008, *Mon. Not. Roy. Astron. Soc.*, 388, 242
- Guy J., et al., 2010, *Astron. Astrophys.*, 523, A7
- Hansen F. K., Banday A. J., Gorski K. M., 2004, *Mon. Not. Roy. Astron. Soc.*, 354, 641
- Heneka C., Marra V., Amendola L., 2014, *Mon. Not. Roy. Astron. Soc.*, 439, 1855
- Hinshaw G., et al., 2013, *Astrophys. J. Suppl.*, 208, 19
- Hutsemekers D., Lamy H., 2001, *Astron. Astrophys.*, 367, 381
- Hutsemekers D., Cabanac R., Lamy H., Sluse D., 2005, *Astron. Astrophys.*, 441, 915
- Javanmardi B., Porciani C., Kroupa P., Pflamm-Altenburg J., 2015, *Astrophys. J.*, 810, 47
- Kalus B., Schwarz D. J., Seikel M., Wiegand A., 2013, *Astron. Astrophys.*, 553, A56
- Kim J., Naselsky P., 2010a, *Astrophys. J.*, 714, L265
- Kim J., Naselsky P., 2010b, *Phys. Rev.*, D82, 063002
- Kim J., Naselsky P., 2011, *Astrophys. J.*, 739, 79
- King J. A., Webb J. K., Murphy M. T., Flambaum V. V., Carswell R. F., Bainbridge M. B., Wilczynska M. R., Koch F. E., 2012, *Mon. Not. Roy. Astron. Soc.*, 422, 3370
- Lewis A., Bridle S., 2002, *Phys. Rev.*, D66, 103511
- Li X., Lin H.-N., 2017, *Chin. Phys.*, C41, 065102
- Li X., Lin H.-N., Wang S., Chang Z., 2015, *Eur. Phys. J.*, C75, 181
- Li X., Zhao S.-P., Tang L., Lin H.-N., 2019, *Commun. Theor. Phys.*, 71, 421
- Lin H.-N., Wang S., Chang Z., Li X., 2016a, *Mon. Not. Roy. Astron. Soc.*, 456, 1881
- Lin H.-N., Li X., Chang Z., 2016b, *Mon. Not. Roy. Astron. Soc.*, 460, 617
- Lineweaver C. H., Tenorio L., Smoot G. F., Keegstra P., Banday A. J., Lubin P., 1996, *Astrophys. J.*, 470, 38
- Mariano A., Perivolaropoulos L., 2012, *Phys. Rev.*, D86, 083517
- Molaro P., et al., 2013, *Astron. Astrophys.*, 555, A68
- Perlmutter S., et al., 1999, *Astrophys. J.*, 517, 565
- Quartin M., Notari A., 2015, *JCAP*, 1501, 008
- Riess A. G., et al., 1998, *Astron. J.*, 116, 1009
- Salehi A., Aftabi S., 2016, *JHEP*, 09, 140
- Salehi A., Setare M. R., 2017, *Gen. Rel. Grav.*, 49, 147
- Schwarz D. J., Weinhorst B., 2007, *Astron. Astrophys.*, 474, 717
- Scolnic D. M., et al., 2018, *Astrophys. J.*, 859, 101
- Sun Z. Q., Wang F. Y., 2018a, *arXiv:1804.05191*
- Sun Z. Q., Wang F. Y., 2018b, *Mon. Not. Roy. Astron. Soc.*, 478, 5153
- Suzuki N., et al., 2012, *Astrophys. J.*, 746, 85
- Tegmark M., de Oliveira-Costa A., Hamilton A., 2003, *Phys. Rev.*, D68, 123523
- Tripp R., 1998, *Astron. Astrophys.*, 331, 815
- Wang J. S., Wang F. Y., 2014, *Mon. Not. Roy. Astron. Soc.*, 443, 1680
- Wang Y. Y., Wang F. Y., 2018, *Mon. Not. Roy. Astron. Soc.*, 474, 3516
- Webb J. K., King J. A., Murphy M. T., Flambaum V. V., Carswell R. F., Bainbridge M. B., 2011, *Phys. Rev. Lett.*, 107, 191101
- Yang X., Wang F. Y., Chu Z., 2014, *Mon. Not. Roy. Astron. Soc.*, 437, 1840
- Zhao W., 2014, *Phys. Rev.*, D89, 023010
- Zhao W., Wu P. X., Zhang Y., 2013, *Int. J. Mod. Phys.*, D22, 1350060
- Zhou Y., Zhao Z.-C., Chang Z., 2017, *Astrophys. J.*, 847, 86